Available online at www.sciencedirect.com
SCIENCE DIRECT®
Journal of Power Sources 130 (2004) 227–232
JOURNAL OF POWER SOURCES
www.elsevier.com/locate/jpowsour

Electrochemical and structural characteristics of metal oxide-coated lithium manganese oxide (spinel type) Part I. In the range of 2.5–4.2 V

Seung-Won Lee [a], Kwang-Soo Kim [a], Hee-Soo Moon [a], Jae-Pil Lee [a], Hyun-Joong Kim [b], Byung-Won Cho [b], Won-Il Cho [b], Jong-Wan Park [a,c,*]

[a] *Division of Materials Science and Engineering, Hanyang University, 17 Haengdang-Dong, Seongdong-Gu, Seoul 133-791, South Korea*
[b] *Nano-Eco Research Center, Korea Institute of Science and Technology, P.O. Box 131, Cheongryang, Seoul 136-791, South Korea*
[c] *Research Center for Energy Conversion and Storage, San 56-1, Shilim-dong, Kwanak-Gu, Seoul 151-742, South Korea*

Received 30 October 2003; accepted 24 November 2003

Abstract

The electrochemical and structural characteristics of the metal oxide-coated spinel were investigated in the range of 2.5–4.2 V. Metal oxide coating on commercial spinel powder ($LiMn_{2-x}M_xO_4$, M = Zr, Nikki, Japan) was carried out using the sol–gel method. Al_2O_3/(PtO_x or CuO_x)-coated spinel exhibited improved cyclability compared to bare spinel. Impedance analysis results indicated that electrochemical resistance value was not consistent with cycle performance. The improved cycle performance of metal oxide-coated spinel may be due to formation of a new $Li_2Mn_4O_9$, Li_2MnO_3 phase, which is expected to have stability to phase transition (Jahn–Teller distortion).

Keywords: Li-ion battery; Lithium manganese oxide; Spinel; Aluminum oxide; Metal oxide coating; Surface treatment

1. Introduction

The layered oxides, $LiCoO_2$, $LiNiO_2$ and spinel $LiMn_2O_4$, have been widely studied as 4 V cathode material. Among these, spinel lithium manganese oxide presents advantages in terms of low cost, easy preparation and environmental friendliness. The main disadvantage of $LiMn_2O_4$ is the loss of capacity during charge–discharge, especially at elevated temperatures. The reason for capacity fading is attributed to several factors: Jahn–Teller distortion [1–3], spinel dissolution [4,5], and electrolyte oxidation [6,7].

Especially in the 3 V region, a large capacity loss is encountered since Jahn–Teller distortion, due to the reduction of the average oxidation state of Mn from 3.5 to 3.0, changes the crystal symmetry from cubic to tetragonal during Li^+ intercalation. The transformation leads to a volume change that is sufficiently large to destroy the structural integrity of the material. To reduce the Mn^{3+} content in $LiMn_2O_4$, the substitution of a small amount of dopant ions at the Mn sites has been proposed as a successful way of improving the cycling stability of $LiMn_2O_4$ [8–13].

In previous reports, researchers such as Amatucci et al. have proposed a surface treatment by using organic and inorganic compounds to decrease the reactivity of the interface between electrode and electolyte [14]. Recently, metal oxide-coated cathodes [15–17] have been shown to exhibit relatively good capacity retention without decrease in the original capacity in severe conditions (for example, a wide charge–discharge range).

We report the preparation of Al_2O_3-coated or Al_2O_3/(PtO_x or CuO_x)-coated spinel by using chloride compounds which may dissolve the spinel element a little during the coating process. As for the Li^+ extraction reaction, Feng et al [18] postulated that the redox-type reaction occurs predominantly for the spinel. This mechanism is based on a surface disproportionation reaction of the two trivalent ions (Mn^{3+}). The ions are soluble in the acid solution under low pH conditions and the Mn^{4+} ions remain in the lattice, forming MnO_2.

$$2Mn^{3+} \rightarrow Mn^{2+} + Mn^{4+}$$

Therefore, it is quite possible that spinel treated with acidic sol solution may comprise a new surface and structure

* Corresponding author. Tel.: +82-2-2290-0386; fax: +82-2-2298-2850.
E-mail address: jwpark@hanyang.ac.kr (J.-W. Park).

0378-7753/$ – see front matter © 2004 Elsevier B.V. All rights reserved.
doi:10.1016/j.jpowsour.2003.11.061

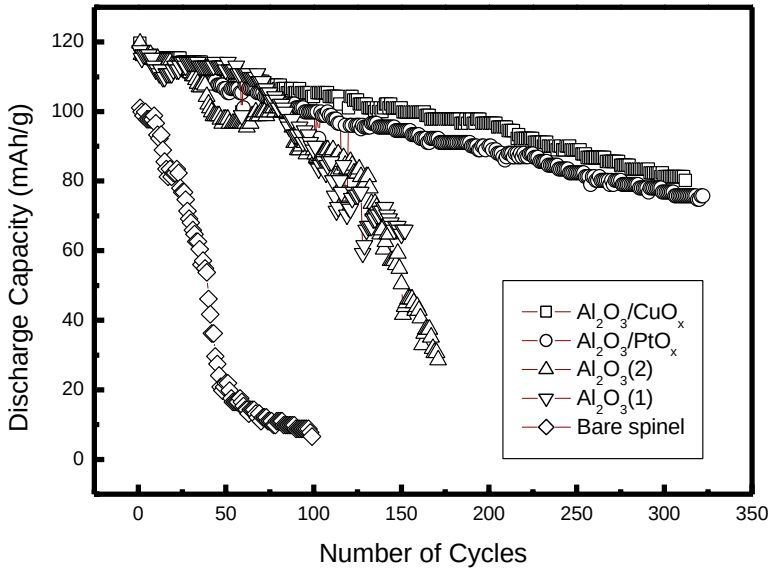

Fig. 1. Cycling behavior of spinel/MCMB cell (*C*-rate: *C*/2, 2.5–4.2 V).

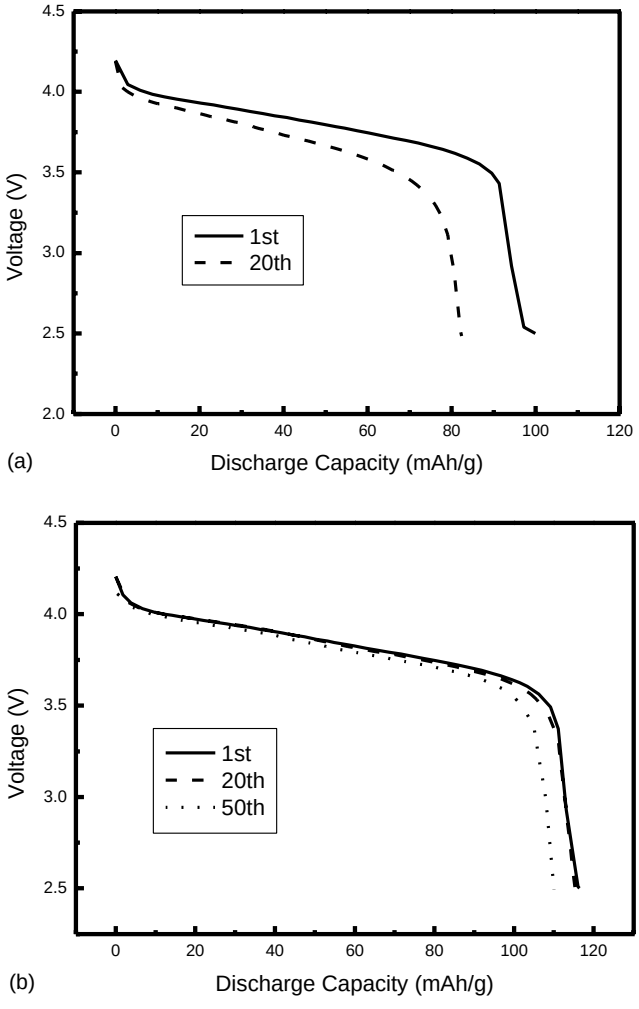

Fig. 2. Discharge profile of spinel/MCMB cell: (a) bare spinel; (b) Al_2O_3/CuO_x-coated spinel.

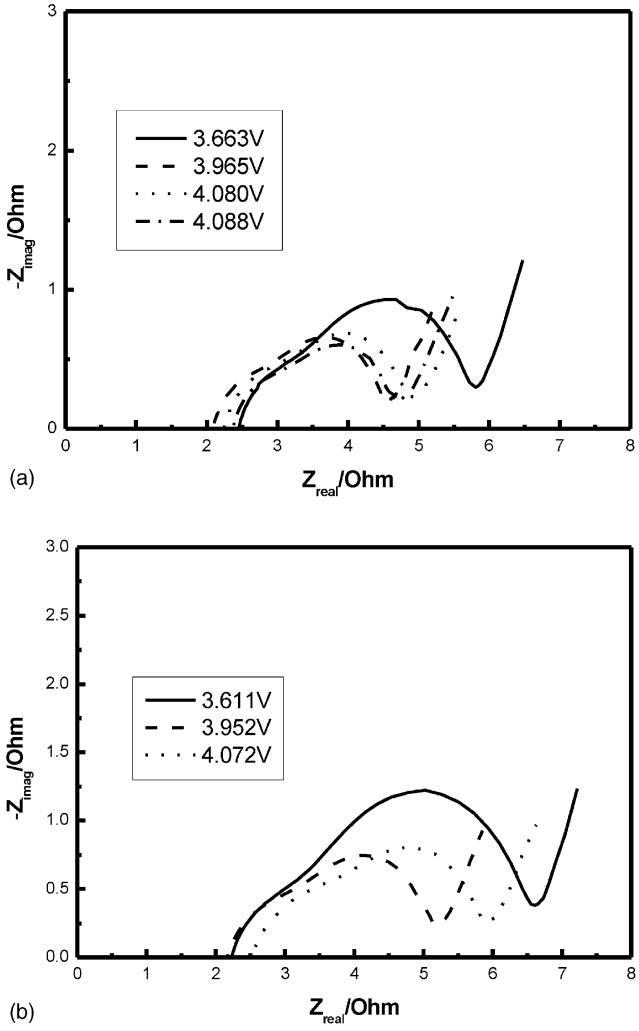

Fig. 3. The ac impedance Nyquist plot of bare spinel/MCMB cell: (a) after 20 cycles; (b) after 30 cycles.

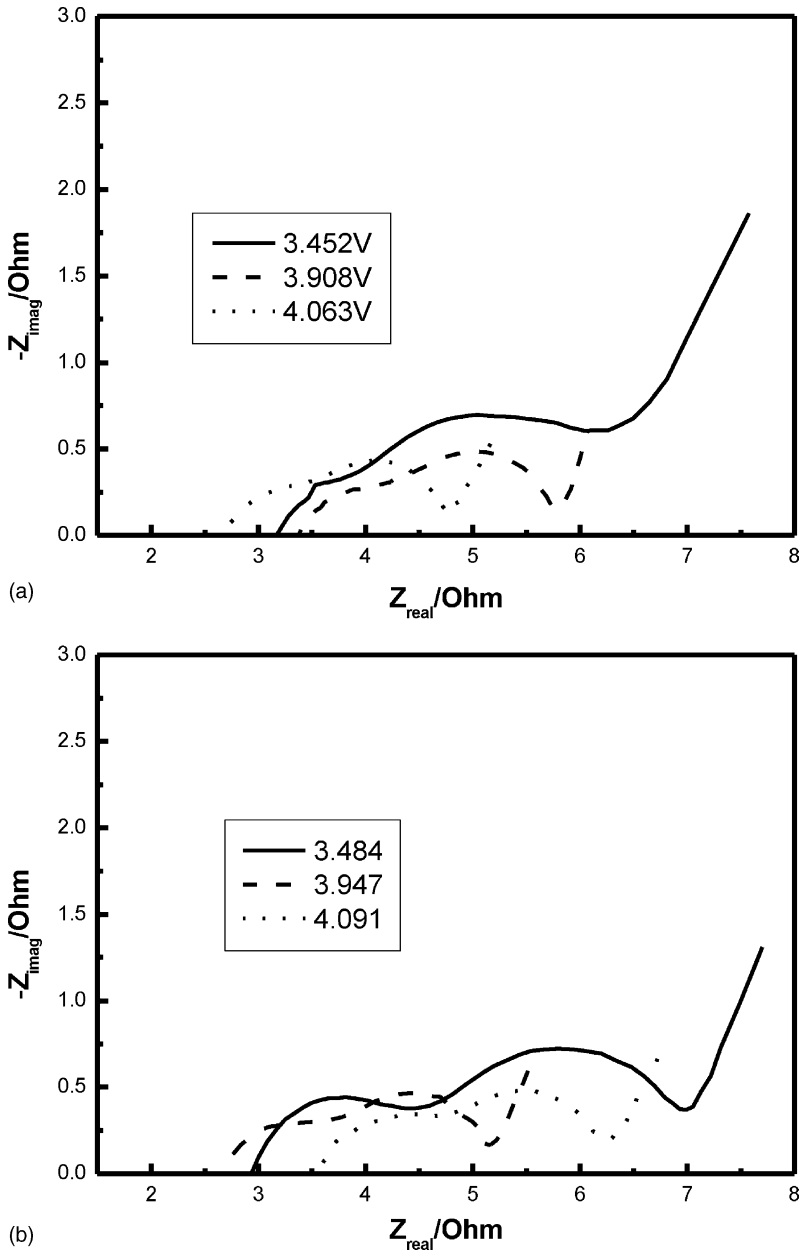

Fig. 4. The ac impedance Nyquist plot of Al_2O_3/CuO_x-coated spinel/MCMB cell: (a) after 100 cycles; (b) after 220 cycles.

after heat treatment. We investigated the electrochemical characteristics and structural properties of Al_2O_3-coated or $Al_2O_3/(PtO_x$ or $CuO_x)$-coated spinel.

2. Experimental

Two sol precursors (0.355 and 0.71 M) for Al_2O_3 coating with spinel powder were prepared by mixing ethyl alcohol and $AlCl_3{\cdot}6H_2O$ (Junsei, Japan). Next, $LiMn_{2-x}M_xO_4$ (Nikki, Japan, M = Zr) was immersed in these sol precursors. To reduce dissolution of manganese attributable to the too low pH of the sol precursor, the immersion time was kept at a few seconds. After drying at 80 °C, the powderobtained

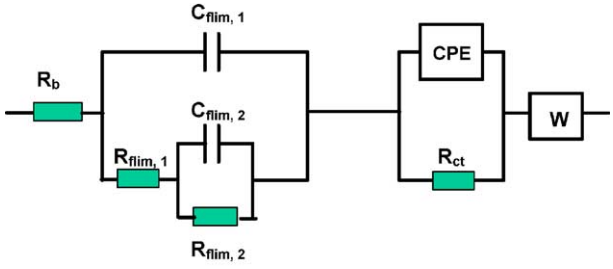

Fig. 5. Proposed equivalent circuit for spinel/MCMB cell.

Table 1
Charge transfer resistance (Ω) with cycling and depth of charging

	Depth of charging (→)			
At 60 cycles				
Al_2O_3/CuO_x	1.007	1.046	1.101	1.156
Al_2O_3/PtO_x	1.006	1.091	1.095	1.159
Al_2O_3(2)	0.9182	1.222	1.317	1.335
Al_2O_3(1)	1.213	1.342	0.8942	–
At 100 cycles				
Al_2O_3/CuO_x	–	1.124	1.015	–
Al_2O_3/PtO_x	–	2.505	2.741	–
Al_2O_3(2)	1.023	1.142	1.505	–
Al_2O_3(1)	1.32	2.158	2.048	–
At 220 cycles				
Al_2O_3/CuO_x	1.879	1.254	1.441	–
Al_2O_3/PtO_x	5.655	6.134	5.885	–
Al_2O_3(2)[a]	3.354	3.458	4.709	3.601
Al_2O_3(1)[a]	1.782	2.126	2.059	–

[a] At 150 cycles.

was heated at 500 °C for 3 h. After being washed with water, it was filtered and then dried at 80 °C. For convenience, each Al_2O_3-coated spinel was named after the concentration ratio of the sol precursor, Al_2O_3(1), Al_2O_3(2). $Al_2O_3/(PtO_x$ or $CuO_x)$-coated powder was prepared as follows: aluminum sol (0.355 M)-coated powder was heated to 150 °C under air, then cooled at room temperature. After additional sol (including $CuCl_2{\cdot}2H_2O$ or $H_2PtCl_6{\cdot}6H_20$) coating, it was heated and filtered in the same way.

XRD measurements were done by means of a diffractometer using Cu Kα radiation. Active materials were mixed with acethylene black and polyvinylidene fluoride (PVdF) using acetone. The slurry was spread on the aluminum foil current collector, followed by pressing and drying. The electrolyte was a mixture of ethylene carbonate (EC), dimethylecarbonate (DMC) and ethylmethylcarbonate (EMC) containing 1 M $LiPF_6$ salt. Electrochemical behavior was determined in a $LiMn_{2-x}M_xO_4$ (M = Zr)/MCMB (as anode) cell sealed in a metallized plastic bag. Impedance spectroscopy was used to determine the dominant factor for electrochemical properties on repeated cycling. Charge/discharge tests were performed galvanostatically at a *C*/2 rate (2.5–4.2 V) in a multi-channel battery tester.

Table 2
Double-layer capacitance (μF) with cycling and depth of charging

	Depth of charging (→)			
At 60 cycles				
Al_2O_3/CuO_x	58.42	53.71	45.86	42.14
Al_2O_3/PtO_x	83.88	66.82	67.82	58.26
Al_2O_3(2)	71.09	28.95	25.14	24.34
Al_2O_3(1)	33.31	26.63	65.93	–
At 100 cycles				
Al_2O_3/CuO_x	–	53.76	59.82	–
Al_2O_3/PtO_x	–	12.72	11.1	–
Al_2O_3(2)	63.65	38.87	23.32	–
Al_2O_3(1)	26.94	11.68	12.45	–
At 220 cycles				
Al_2O_3/CuO_x	17.79	32.14	27.89	–
Al_2O_3/PtO_x	1.793	1.631	1.664	–
Al_2O_3(2)[a]	5.8	4.721	3.023	3.873
Al_2O_3(1)[a]	11.55	7.93	8.116	–

[a] At 150 cycles.

3. Results and discussion

To evaluate cycling performance of the spinel/MCMB cell in the range from 2.5 to 4.2 V, the discharge capacity as a function of the number of cycles is shown in Fig. 1. The discharge capacity of the bare spinel rapidly faded during cycling. This may be directly related to structural breakdown due to Jahn–Teller distortion. Although Al_2O_3-coated spinel gives stable cycle characteristics compared to bare spinel, the capacity declines upon cycling too. However, $Al_2O_3/(PtO_x$

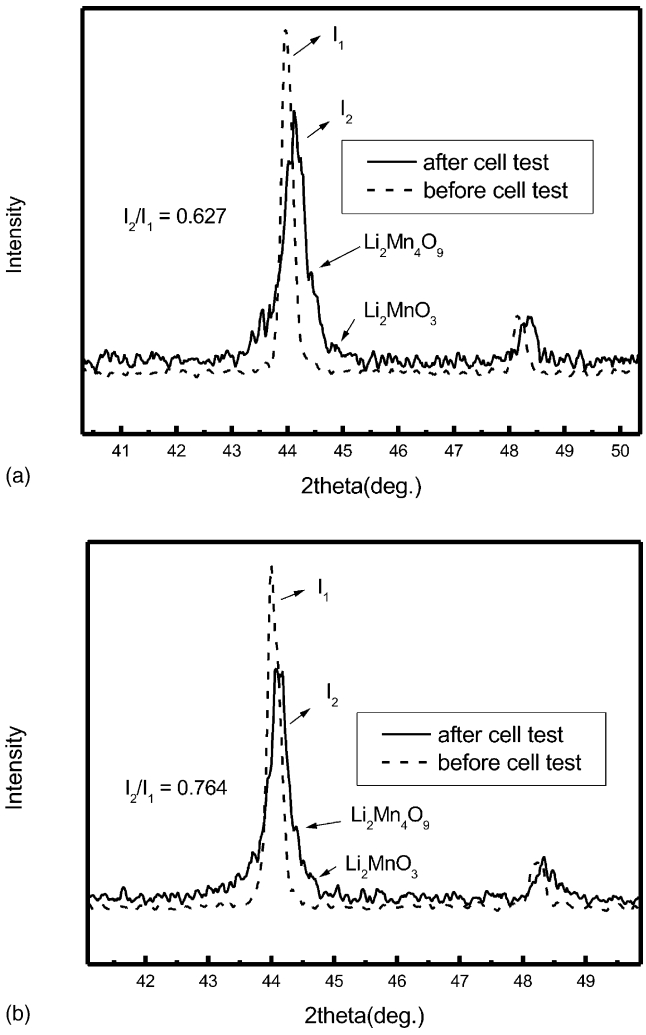

Fig. 6. X-ray diffraction of Al_2O_3/CuO_x-coated spinel and Al_2O_3/PtO_x-coated spinel before and after cell test: (a) Al_2O_3/CuO_x-coated spinel; (b) Al_2O_3/PtO_x-coated spinel.

or CuO_x)-coated spinel exhibited improved cyclability. In general, the discharge curve of the $Li/Li_xMn_2O_4$ cell exhibits two voltage plateaus. In the range $0 \leq x \leq 1$, the cell discharges at 4 V versus Li/Li^+, whereas in the range $1 \leq x \leq 2$, the cell discharges at 3 V versus Li/Li^+.

The discharge profile of bare spinel (for 1st and 20th) and Al_2O_3/CuO_x-coated spinel (for 1st, 20th and 50th) are shown in Fig. 2. The plateau which suggests the existence of two phases arising from the Jahn–Teller distortion was not observed, but the discharge profile of bare spinel revealed fast degradation during subsequent cycling.

In order to evaluate the electrochemical resistance of bare spinel and Al_2O_3/CuO_x-coated spinel with cycling, ac impedance spectroscopy as a function of voltage was carried out at 20 and 30 cycles (for bare spinel, Fig. 3) and 100 and 220 cycles (for Al_2O_3/CuO_x-coated spinel, Fig. 4). There are two semi-circles that indicate surface resistance and charge transfer resistance, respectively. In spite of more a progressed cycle number, Al_2O_3/CuO_x-coated spinel has lower charge transfer resistance than bare spinel.

By employing an equivalent circuit (Fig. 5) of the spinel/MCMB cell to simulate impedance data, a list of the charge transfer resistance (Rct) and constant phase elements (CPE) with cycling and depth of charging are given in Tables 1 and 2. With an increasing number of cycles and depth of charging, Rct and CPE of the spinel sample increased and decreased, respectively, but Al_2O_3/CuO_x-coated spinel has lower electrochemical resistance than the other samples, which is consistent with cycle performance. However, after 220 cycles, Al_2O_3/PtO_x-coated spinel is highly resistive, despite relatively small capacity fade. Therefore, it has been concluded that the main reason for capacity

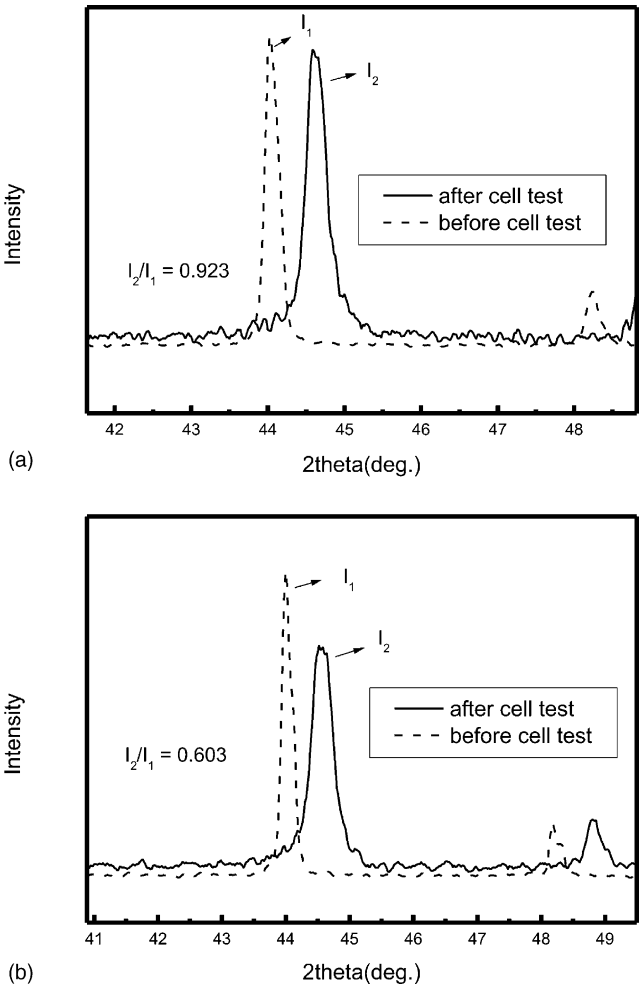

Fig. 7. X-ray diffraction of $Al_2O_3(1)$ and $Al_2O_3(2)$-coated spinel before and after cell test: (a) $Al_2O_3(1)$-coated spinel; (b) $Al_2O_3(2)$-coated spinel.

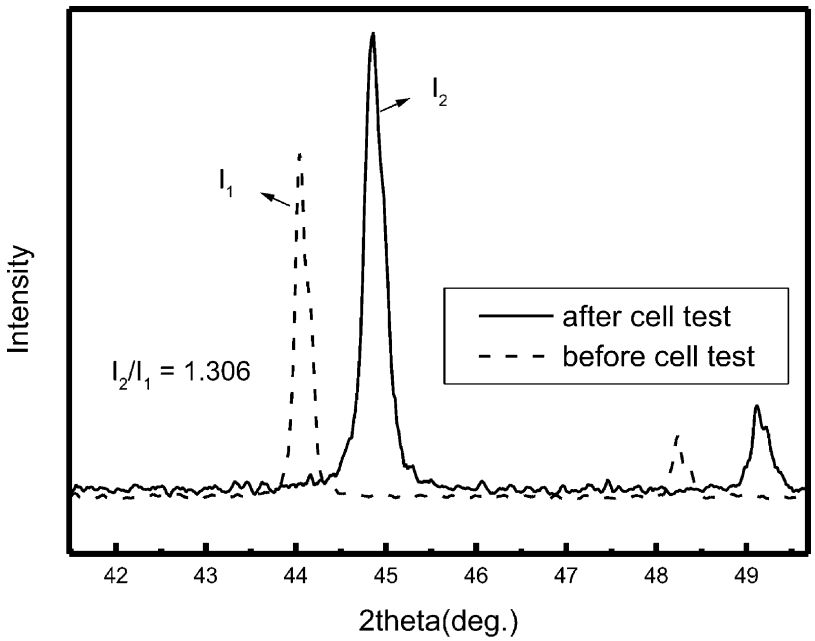

Fig. 8. X-ray diffraction of bare spinel before and after cell test.

fading may be the structural change of the spinel rather than the increase of electrochemical resistance.

In order to investigate the structural change of the spinel after the cell test, XRD studies were carried out (Figs. 6–8). The ratio of [4 0 0] intensity (basis: [1 1 1] intensity = 100) before and after the cell test was marked in Figs. 6–8. From Figs. 6 and 7, it is noted that a new phase [19] ($Li_2Mn_4O_9$, Li_2MnO_3) and the peak broadening are observed after the cell test in the range of 2.5–4.5 V. The improved cycle performance of Al_2O_3/(PtO_x or CuO_x)-coated spinel may be due to the $Li_2Mn_4O_9$, Li_2MnO_3 phase, which is expected to have stability to phase transition (Jahn–Teller distortion) because $Li_2Mn_4O_9$ and Li_2MnO_3 are composed entirely of Mn^{4+}. I_2/I_1 (the ratio of [4 0 0] intensity before and after the cell test) is found to be 0.627 and 0.764, respectively. Fig. 7 presents the XRD pattern of Al_2O_3(1) and Al_2O_3(2) samples after the cell test. The result obtained is different from that in the Fig. 6 from the point of view of peak shifting and the lack of a new peak.

Fig. 8 shows the XRD pattern of bare spinel after the cell test. Peak shifting to a high angle is observed and the ratio of I_2/I_1 increased in contrast to other samples. This means the collapse of the lithium insertion–extraction path caused by relative decrease of [1 1 1] (main peak) intensity.

4. Conclusions

A discharge plateau, which suggests the existence of two phases arising from the Jahn–Teller distortion was not observed, but the discharge profile of bare spinel revealed fast degradation during subsequent cycling. However, Al_2O_3/(PtO_x or CuO_x)-coated spinel exhibited improved cyclability. This is due to the formation of a new phase which is expected to have stability to phase transition.

Acknowledgements

This work was supported by KOSEF through the Research Center for Energy Conversion and Storage.

References

[1] R.J. Gummow, A. de Kock, M.M. Thackeray, Solid State Ionics 69 (1994) 59.
[2] M.M. Thackeray, Y. Shao-Horn, A.J. Kahaian, Electrochem. Solid-State Lett. 1 (1998) 7.
[3] A. Yamada, M. Tanaka, K. Tanaka, K. Sekai, J. Power Sources 81–82 (1999) 73.
[4] D.H. Jang, S.M. Oh, Electrochim. Acta 43 (1998) 1023.
[5] T. Aoshima, K. Okahara, C. Kiyohara, K. Shizuka, J. Power Sources 97–98 (2001) 377.
[6] D.H. Jang, J.S. Young, S.M. Oh, J. Electrochem. Soc. 143 (1996) 2204.
[7] Y. Gao, J.R. Dahn, Solid State Ionics 84 (1996) 33.
[8] C.H. Shen, R.S. Liu, R. Gundakaram, J.M. Chen, S.M. Huang, J.S. Chen, C.M. Wang, J. Power Sources 102 (2001) 21.
[9] M. Wohlfahrt-Mehrens, A. Butz, R. Oesten, J. Power Sources 68 (1997) 582.
[10] A.D. Robertson, S.H. Lu, W.F. Howard, J. Electrochem. Soc. 144 (1997) 3500.
[11] P. Arora, B.N. Popov, R.E. White, J. Electrochem. Soc. 145 (1998) 807.
[12] M. Yoshio, Y. Xia, N. Kumada, S. Ma, J. Power Sources 101 (2001) 79.
[13] C.S. Yoon, C.K. Kim, Y.-K. Sun, J. Power Sources 109 (2002) 234.
[14] G.G. Amatucci, A. Blyr, C. Sigala, P. Alfonse, J.M. Tarascon, Solid State Ionics 104 (1997) 13.
[15] H.-J. Kweon, D.G. Park, Electrochem. Solid-State Lett. 3 (2000) 128.
[16] H.-J. Kweon, S.J. Kim, D.G. Park, J. Power Sources 88 (2000) 255.
[17] J. Cho, Y.J. Kim, B. Park, Chem. Mater. 12 (2000) 3788.
[18] Q. Feng, Y. Miyai, H. Kanoh, K. Ooi, Langmuir 8 (1992) 1861.
[19] A. Blyr, C. Sigala, G. Amatucci, D. Guyomard, Y. Chabre, J-M. Tarascon, J. Electrochem. Soc. 145 (1998) 194.